Available online at www.sciencedirect.com

ScienceDirect

Journal of Ocean Engineering and Science 2 (2017) 5–17

www.elsevier.com/locate/joes

Original Article

Fully enclosed multi-axis inertial reaction mechanisms for wave energy conversion

I.A. Antoniadis, V. Georgoutsos, A. Paradeisiotis*

Mechanical Design and Control Systems Section, Mechanical Engineering Department, National Technical University of Athens, Heroon Polytechniou 9, Zografou 15780, Greece

Received 9 October 2016; received in revised form 5 February 2017; accepted 9 February 2017
Available online 22 February 2017

Abstract

This paper introduces a novel concept for wave energy conversion, using fully enclosed appropriate internal body configurations, which provide inertial reaction against the motion of an external vessel. In this way, reliability, robustness and survivability under extreme weather conditions – a fundamental prerequisite for wave energy converters – can be achieved. Acting under the excitation of the waves, the external vessel is subjected to a simultaneous surge and pitch motion in all directions, ensuring maximum wave energy capture in comparison to other wave energy converters like point heave absorbers. The internal body is suspended from the external vessel body in such an appropriate geometrical configuration, that a symmetric four-bar mechanism is essentially formed. The main advantage of this suspension geometry is that a linear trajectory results for the centre of the mass of the suspended body with respect to the external vessel, enabling the introduction of a quite simple form of a Power Take Off (PTO) design. Thus, because of this simplicity and symmetry of the suspension geometry and of the PTO mechanism, the fundamental restrictions of other linear, pendulum or gyroscopic variants on inertial reacting bodies are significantly removed.

Keywords: Waves; Energy; Inertial; Pendulum; Platforms; Offshore.

1. Introduction

Oceans constitute more than 75% of our planet and the waves being produced in them consist one of the biggest untapped renewable energy resources of our world. Various estimates and methodologies with varying figures exist [1–3], converging however to estimates for a wave power exceeding 2 TW, which is of the same order as global electricity production. Much higher perspectives exist in the hybrid wind-wave energy exploitation. Using only North Sea sites with water over 50 m deep as an example, the energy produced in this area could meet today's EU electricity consumption four times over [4,5]. An additional potential exists in suitable areas of the Atlantic and Mediterranean seas. This fact has inspired numerous inventors, as early as 1799. The main systematic research effort for efficient wave energy converters was only stimulated by the emerging oil crisis of the 1970s. As a result, more than a thousand of patents and tens (if not hundreds) of experimental prototypes are being tested in the sea. Some comprehensive recent reviews can be found in [6–8]. However, contrary to the case of the Horizontal Axis Wind Turbine (HAWT) for wind energy conversion, no specific technological paradigm exists till today for efficient wave energy conversion. As a result, numerous varieties of wave energy converters exist, such as oscillating water columns, attenuators, and point absorbers in the form of heaving buoys, overtopping devices, and oscillating flap wave devices being among the most common. However, their Technological Readiness Levels (TRLs) and overall efficient performance is still quite low.

One reason is the very short past of 40 years of systematic research for wave energy conversion, compared to the hundreds (if not thousands) of years of wind energy technology. Another reason are the difficulties in understanding the wave energy absorption process, involving complex hydrodynamic

* Corresponding author.
E-mail address: aparadis@mail.ntua.gr (A. Paradeisiotis).

http://dx.doi.org/10.1016/j.joes.2017.02.003

phenomena, such as wave diffraction and radiation, although significant progress has been achieved the last 40 years towards this direction.

Today, the main obstacles for efficient wave energy conversion are mainly related to the requirement for survivability in extreme weather conditions, and to the energy efficient and reliable design of the PTO mechanism. This last requirement involves not so much the design of the PTO device itself, but much more its seamless and energy efficient interface and integration with the wave absorption vessel and the electrical grid.

Towards the last direction, numerous concepts of wave energy converter systems have been conceived, consisting from two-body configurations, in which only one body is in contact with the water and the other body is located above the water or is totally enclosed inside the wetted one. This design enables such mechanisms to fulfil in the best possible way a fundamental prerequisite for wave energy converters: the requirement for reliability, robustness and survivability under extreme weather conditions.

The earliest example in this direction are perhaps the Frog and PS Frog designs at the University of Lancaster in England [9,10]. Frog actually refers to a heaving absorber, while PS Frog refers to a combined surging and pitching absorber, all actually resulting to a PTO mechanism in the form of a linear sliding mass, enclosed inside a floating vessel. Parallel, an approach for the theoretical modelling and control of such devices has been performed in [11,12], essentially for the heaving ones. An interesting variant of this design, acting essentially in the form of a vertical pendulum has been proposed: the SEAREV [13] concept. The basic disadvantages of these two designs consist in their limited capability for wave capture in a single axis and in the big masses they require for efficient energy capture, thus demanding complex and unreliable support structures.

Other designs in the forms of an inverted pendulum have been proposed [14], which however result to unstable structures, possibly extended quite high above the sea level. Parallel, horizontal pendulum designs [15,16] have been proposed, which however introduce problems of stability of the external vessel, only partially compensated by asymmetric ballast designs. Quite recently, the GAIA multi-axis wave energy converter has been also proposed [17]. However, it still requires a complicated support structure and PTO mechanisms.

An interesting variant of such concepts is the class of designs, which make use of a gyroscope as an internal reacting inertial configuration [18–22]. However, no systematic analysis exists on the requirements for significant energy capture by such designs, in terms of rotating masses and corresponding speeds. Furthermore, their complexity consists a further serious disadvantage for their reliability and robustness in the harsh sea environments.

This paper introduces a novel concept for the design of a general class of fully enclosed internal body configurations, providing inertial reaction against the motion of an external vessel, able to drastically overcome the disadvantages of the above designs. Acting under the excitation of the waves, the external vessel can perform in general a 6 degrees of freedom arbitrary translation and rotation of in space.

The internal bodies are suspended from the external body in such appropriate geometrical configurations, that the entire assembly of the internal and external bodies, together with their suspension systems, form essentially a multi-link mechanism. The kinematic design of these mechanisms can be performed in such a way, that the internal bodies can follow a well prescribed relative motion with respect to the external body. Moreover, each individual body has an optimal mass and inertia distribution.

This overall design enables the maximum conversion and storage of wave energy from all the degrees of freedom of the external body, into the form of kinetic and potential energy, stored into the total assembly of the internal bodies. Moreover, since specific points of the internal body assembly can be arranged to follow prescribed trajectories with respect to the external vessel, simple and established forms of power take off systems can be appropriately inserted (linear or rotary, hydraulic or electrical), in order to further convert the internally stored mechanical energy to electrical energy.

An example of such an arrangement is further analysed in details in the rest of this paper. An external vessel is subjected to simultaneous surge and pitch motion in all directions, ensuring thus maximum wave capture, in comparison for e.g. to heave only point absorbers. An inertial reacting body is enclosed internally, suspended appropriately from the external body in such a way that a symmetric four-bar mechanism is formed.

The first advantage of this suspension geometry is that the centre of the mass of the suspended body moves in a linear trajectory with respect to the external vessel. This implies the internal body appears to move essentially in linear way, like a simple mass in the conventional form of the PSFrog arrangements. This enables the introduction of a quite simple Power Take Off (PTO) system, as for e.g. hydraulic rams. Moreover, the simplicity and the symmetry of the suspension geometry and of the PTO, ensure a quite simple and robust technological implementation, contrary to all other known above variants of inertial reacting internal bodies.

The second advantage of this design is that the internal body behaves dynamically as a vertically suspended pendulum. However, the suspension geometry, in combination to the optimal mass and the inertia distribution of the internal body, ensure the maximal conversion and storage of the wave energy in the form of kinetic and potential energy. This is reflected to the resulting equivalent pendulum length and inertia of this design, which can far exceed those that can be achieved by an actual technical implementation either of a simple horizontal or of a vertical pendulum (suspended, or inverted). The direct consequence is significant reduction of the suspended mass.

The kinematic relations and the dynamic equations of motion are derived in Section 2. In Section 3 the equations of motion are linearised, an appropriate feedback law is proposed and the power that can be converted is estimated. Finally an indicative design is presented in Section 4, as a standalone

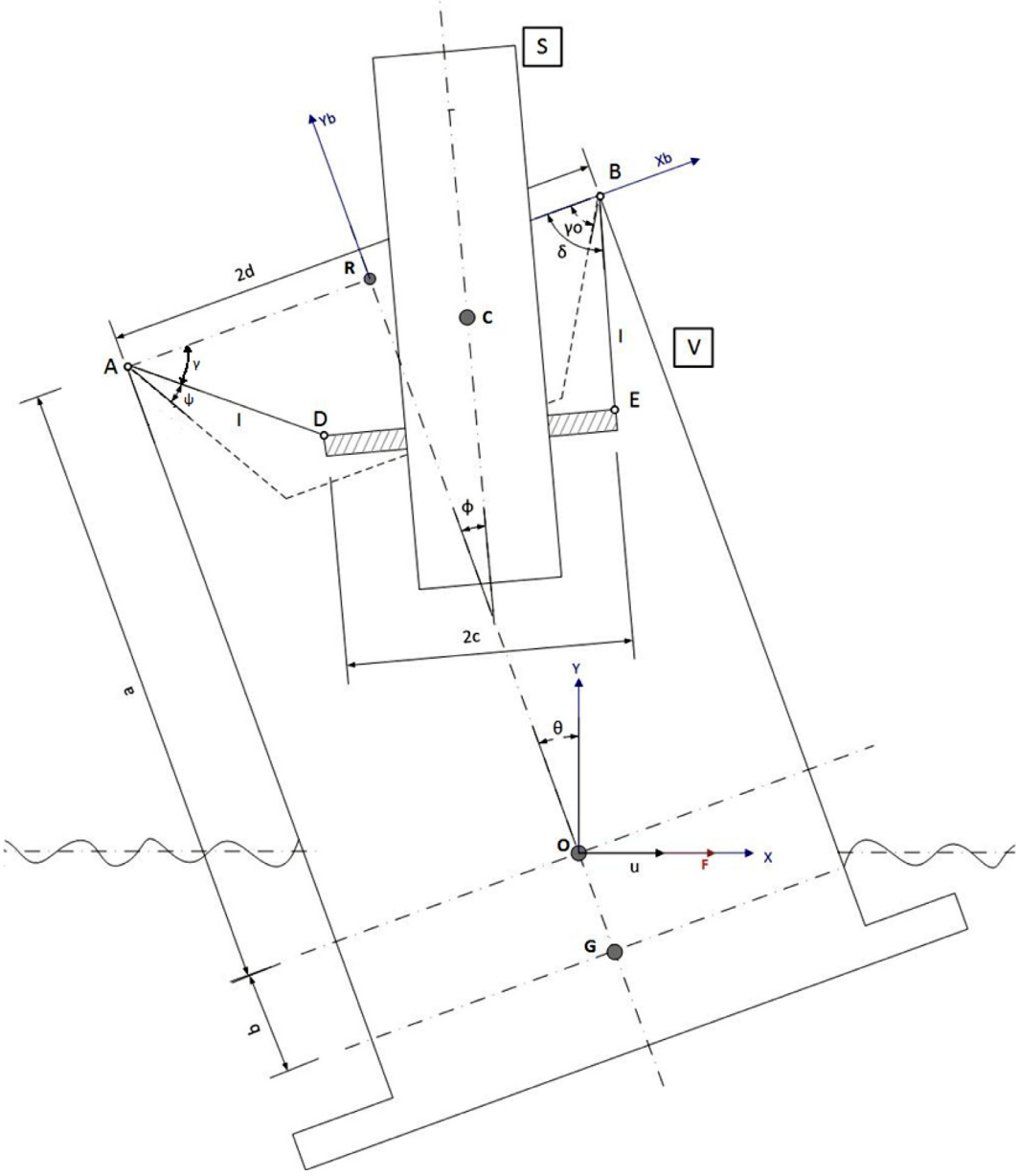

Fig. 1. Schematic presentation of the assembly considered. An internally reacting body *S* is suspended by an appropriate mechanism from an external floating vessel *V*.

750 kW rated power configuration. In Section 5, the standout features of this novel design along with the conclusions from the dynamical analysis and the indicative implementation are summarised.

2. Equations of motion

2.1. Description of the assembly and basic definitions

The assembly considered, is depicted in Fig. 1, consisting from a floating external vessel *V*, into which an internal four-bar mechanism *ABDE* is hoisted. The waves induce to the vessel, a simultaneous surge motion of magnitude u and a pitching motion of an angle θ, with respect to the inertial coordinate system *OXY*. The origin *O* is located at the intersection of the level of the sea with the vertical axis of symmetry of the vessel. The centre of mass of the vessel *G* is located at a distance b from the point *O* below the level of the sea. The member DE of the internal four-bar mechanism provides a basis onto which a solid body *S* is placed. The solid body provides a reaction mass to the motion of the external vessel, rotating with an angle ϕ about the *Z* axis of the inertial reference frame *OXY*. The initial (rest) position *R* of this solid body's centre of mass, is located on the axis of symmetry of the vessel *V*, at a distance a from the origin *O*. The coordinate reference system RX_bY_b is rigidly attached to the vessel *V*, following its motion.

The form of the mooring system is outside of the scope of this paper, however it is assumed that the mooring forces are sufficient to keep the device on station, but negligible

in comparison with the wave and dynamic forces. The power take off mechanism (e.g. hydraulic rams) is quite simple, so it can be designed to lock – even in a pure mechanical way – the internal oscillating body in a safe position in the case of rough sea conditions. The rest position of the system corresponds to $\theta = \phi = u = 0$

- O: origin of the inertial coordinate system OXY – intersection of the level of the sea with the vertical axis of symmetry of the vessel in the rest position,
- C: centre of mass of the body S,
- R: origin of the body axis system RX_bY_b – initial (rest) position of C,
- G: centre of mass of the vessel V,
- a: distance between R and O,
- b: distance between G and O,
- ϕ: rotating angle of the body S about the Z axis,
- θ: pitching motion induced by the waves,
- u: surge motion induced by the waves.

2.2. Kinematic analysis

The detailed kinematic analysis of the motion of the centre of mass C of the body S with respect to the body fixed frame RX_bY_b is performed in Appendix 1. Also, Fig. 10 shows the geometrical parameters and kinematic variables of the four bar mechanism. The symbols are defined as:

- x_G, y_G: coordinates of the centre of gravity G of the external vessel, with respect to the inertial coordinate system OXY,
- x_B, y_B: coordinates of the centre of gravity C of the suspended mass, with respect to the body fixed coordinate system RX_bY_b,
- x_M, y_M: coordinates of the centre of gravity C of the suspended mass, with respect to the inertial coordinate system OXY.

The displacement and velocity of the point G with respect to the inertial coordinate system OXY are as follows:

$$x_G = u + b\sin\theta \quad [\text{m}] \tag{1}$$

$$y_G = -b\cos\theta \quad [\text{m}] \tag{2}$$

$$\dot{x}_G = \dot{u} + \dot{\theta} b\cos\theta \quad [\text{m/s}] \tag{3}$$

$$\dot{y}_G = \dot{\theta} b\sin\theta \quad [\text{m/s}] \tag{4}$$

The translation of the reaction mass according to the system OXY is as follows:

$$\begin{aligned} x_M &= x_R + x_B\cos\theta - y_B\sin\theta \\ &= u + x_B\cos\theta - (a + y_B)\sin\theta \quad [\text{m}] \end{aligned} \tag{5}$$

$$\begin{aligned} y_M &= y_R + x_B\sin\theta + y_B\cos\theta \\ &= x_B\sin\theta + (a + y_B)\cos\theta \quad [\text{m}] \end{aligned} \tag{6}$$

where:

$$x_R = u - a\sin\theta \quad [\text{m}] \tag{7}$$

$$y_R = a\cos\theta \quad [\text{m}] \tag{8}$$

The corresponding expressions for x_B, y_B are given in Eqs. (A.35) and (A.36).

The expression of the corresponding velocities $\dot{x}_M$ and $\dot{y}_M$ result as follows:

$$\dot{x}_M = \dot{u} - l_{x_M}\dot{\theta} + r_{x_M}\dot{\phi} \quad [\text{m/s}] \tag{9}$$

$$\dot{y}_M = l_{y_M}\dot{\theta} + r_{y_M}\dot{\phi} \quad [\text{m/s}] \tag{10}$$

where:

$$l_{x_M} = (a + y_B)\cos\theta + x_B\sin\theta \quad [\text{m}] \tag{11}$$

$$l_{y_M} = x_B\cos\theta - (a + y_B)\sin\theta \quad [\text{m}] \tag{12}$$

$$r_{x_M} = r_x\cos\theta - r_y\sin\theta \quad [\text{m}] \tag{13}$$

$$r_{y_M} = r_x\sin\theta + r_y\cos\theta \quad [\text{m}] \tag{14}$$

and the expressions for $\dot{x}_B, \dot{y}_B$ are given in Eqs. (A.42) and (A.43).

2.3. Dynamic equations of motion

The kinetic energy captured from the bodies can be written as:

$$\begin{aligned} T = {} & \frac{1}{2}m_V(\dot{x}_G^2 + \dot{y}_G^2) + \frac{1}{2}I_V\dot{\theta}^2 + \frac{1}{2}m_s(\dot{x}_M^2 + \dot{y}_M^2) \\ & + \frac{1}{2}I_s(\dot{\theta} - \dot{\phi})^2 \quad \left[\frac{\text{kg m}^2}{\text{s}^2} = \text{J}\right] \end{aligned} \tag{15}$$

where:

- m_v: the mass of the vessel V including the added mass of the water,
- m_s: the mass of the body S,
- I_V: the moment of inertia of the vessel about O,
- I_s: the moment of inertia of the reaction mass about C.

The potential energy is as follows:

$$U = m_s g y_M + \frac{1}{2}K_V\theta^2 + m_V g y_G \quad \left[\frac{\text{kg m}^2}{\text{s}^2} = \text{J}\right] \tag{16}$$

where K_V is the hydrostatic stiffness in pitch (and/or roll) for the vessel about point O, associated with the component of the buoyancy force. The gravitational effect of the vessel is taken into consideration separately.

The device is designed as a surge but not heave energy converter. This implies that it can convert only surge and pitch motions of the external vessel. The heave motion of the internal device is prohibited due to its weight, which will generate significant technical problems. Therefore the system presents three degrees of freedom:

$$r_1 = u \quad [\text{m}], \quad r_2 = \theta \quad [\text{rad}], \quad r_3 = \phi \quad [\text{rad}] \tag{17}$$

The equations of motion of the system can be derived by the application of the following Lagrange principle:

$$\frac{d}{dt}\left(\frac{\partial L}{\partial \dot{r}_i}\right) - \frac{\partial L}{\partial r_i} = F_i, \quad i = 1, 2, 3 \tag{18}$$

$$L = T - U \tag{19}$$

where F_i denotes the external and the damping forces of the system. Using the expressions of derivatives of Appendix A.2, the equations of motion result as:

$$\frac{d}{dt}P_u + R_u\dot{u} = F_w \quad \left[\frac{\text{kg m}}{\text{s}^2} = \text{N}\right] \tag{20}$$

$$\frac{d}{dt}P_\theta + K_v\theta + T_{v\theta} + T_{g\theta} = 0 \quad [\text{Nm}] \tag{21}$$

$$\frac{d}{dt}P_\phi + T_{g\phi} = T_p \quad [\text{Nm}] \tag{22}$$

where the generalised momentum values P_u [kg m/s], P_θ [kg m^2/s], P_ϕ [kg m^2/s] are defined as follows:

$$\begin{Bmatrix} P_u \\ P_\theta \\ P_\phi \end{Bmatrix} = \begin{bmatrix} M_{uu} & M_{u\theta} & M_{u\phi} \\ M_{u\theta} & M_{\theta\theta} & M_{\theta\phi} \\ M_{u\phi} & M_{\theta\phi} & M_{\phi\phi} \end{bmatrix} \begin{Bmatrix} \dot{u} \\ \dot{\theta} \\ \dot{\phi} \end{Bmatrix} \tag{23}$$

with the components of the mass matrix $\mathbf{M}$:

$$M_{uu} = m_v + m_s \quad [\text{kg}] \tag{24}$$

$$M_{u\theta} = m_v b\cos\theta - m_s l_{x_M} \quad [\text{kg m}] \tag{25}$$

$$M_{u\phi} = m_s r_{x_M} \quad [\text{kg m}] \tag{26}$$

$$M_{\theta\theta} = I_v + I_s + m_v b^2 + m_s(l_{x_M}^2 + l_{y_M}^2) \quad [\text{kg m}^2] \tag{27}$$

$$M_{\theta\phi} = -\left[I_s + m_s(r_{x_M} l_{x_M} - r_{y_M} l_{y_M})\right] \quad [\text{kg m}^2] \tag{28}$$

$$M_{\phi\phi} = I_s + m_s(r_{x_M}^2 + r_{y_M}^2) \quad [\text{kg m}^2] \tag{29}$$

The moments due to the gravity are:

$$T_{v\theta} = m_v g b\sin\theta \quad [\text{Nm}] \tag{30}$$

$$T_{g\theta} = m_s g l_{y_M} \quad [\text{Nm}] \tag{31}$$

$$T_{g\phi} = m_s g r_{y_M} \quad [\text{Nm}] \tag{32}$$

The rest of the terms are:

- R_u: an added damping coefficient for the surge motion induced by the waves (radiation force),
- F_w: the force due to the incident and diffracted waves,
- T_p: the reaction moment of the PTO mechanism, proportionate to the angular velocity of the oscillating internal body $\dot{\phi}$.

The water-plane area is taken to be small compared with the frontal area, so that excitation moments in pitch are relatively small, therefore not participating in the model derivation. The part of the radiation force describing the effect of the added mass is incorporated in the expression of the generalised momentum P_u and the added mass is represented as M_{uu} in the mass matrix Eq. (23). The design concept is quite simple, since it foresees that the internal body is suspended from the external body by ropes or equivalent mooring line materials. Therefore, at this preliminary stage, the effects of frictional damping generated from the various connections are considered negligible.

2.4. State space representation

A compact state space representation for the system of equations is possible under the following compact form:

$$\dot{\mathbf{z}}_1 = \mathbf{M}^{-1}\mathbf{z}_2 \tag{33}$$

$$\dot{\mathbf{z}}_2 = \mathbf{f}_R \tag{34}$$

where:

$$\mathbf{z}_1^T = \mathbf{r}^T = \begin{Bmatrix} u & \theta & \phi \end{Bmatrix} \tag{35}$$

$$\mathbf{z}_2^T = \begin{Bmatrix} P_u & P_\theta & P_\phi \end{Bmatrix} \tag{36}$$

$$\mathbf{f}_R = \begin{Bmatrix} F_w - R_u\dot{u} \\ -K_{v\theta} - T_{v\theta} - T_{g\theta} \\ -T_{g\phi} + T_p \end{Bmatrix} \tag{37}$$

2.5. Equation of motion of the internal inertial reacting body

Under the assumption that the surge and pitch motion of the external vessel are known in the time domain, the equations of motion can be further simplified, retaining only the set of equations which refer to the mechanism itself:

$$\frac{d}{dt}(M_{\phi\phi}\dot{\phi}) = -\frac{d}{dt}(M_{u\phi}\dot{u} + M_{\theta\phi}\dot{\theta}) - T_{g\phi} + T_p \quad [\text{Nm}] \tag{38}$$

In an equivalent state space representation:

$$\mathbf{z} = \begin{bmatrix} \phi \\ P_\phi \end{bmatrix} \tag{39}$$

$$\begin{bmatrix} \dot{\phi} \\ \dot{P}_\phi \end{bmatrix} = \begin{bmatrix} (P_\phi - M_{u\phi}\dot{u} - M_{\phi\phi}\dot{\phi})/M_{\phi\phi} \\ -T_{g\phi} + T_p \end{bmatrix} \tag{40}$$

3. Maximum power conversion capability

3.1. Linearisation of the equations of motion

Under the assumption of small perturbations around the rest position of the mechanism, the following approximate relations hold for the angles $\alpha \in \{\phi, \psi, \theta\}$ of the assembly:

$$\cos\alpha \approx 1 \tag{41}$$

$$\sin\alpha \approx \alpha \tag{42}$$

which results to:

$$\cos\gamma = \cos(\gamma_0 - \psi) \approx \cos\gamma_0 + \psi\sin\gamma_0 \tag{43}$$

$$\sin\gamma = \sin(\gamma_0 - \psi) \approx \sin\gamma_0 - \psi\cos\gamma_0 \tag{44}$$

The equations of motion (A.35) and (A.36) of the of the centre of mass C of the oscillating body with respect to the origin

R of the coordinate system RX_bY_b can thus be simplified as follows:

$$x_B \approx l_p\phi \quad [\text{m}] \tag{45}$$

$$y_B \approx 0 \quad [\text{m}] \tag{46}$$

$$l_p = (\mu + 1)h \quad [\text{m}] \tag{47}$$

$$\mu \approx \mu_0 = \frac{2c}{l\sigma_0} = \frac{c}{l\cos\gamma_0} = \frac{1}{d/c - 1} \tag{48}$$

$$\sigma \approx \sigma_0 = \frac{\sin 2\gamma_0}{sin\gamma_0} = 2\cos\gamma_0 \tag{49}$$

Eq. (46) implies that the physical motion of the centre of the mass of the body is linear, exactly in the same way as the traditional designs of linear sliding mass Wave Energy Converters (WECs), as for e.g. in the form of PS Frog. Similar simplified relations hold for the e factors r_x, r_y, l_{x_M}, l_{y_M}, r_{x_M} and ry_M:

$$r_x \approx l_p \quad [\text{m}] \tag{50}$$

$$r_y \approx 0 \quad [\text{m}] \tag{51}$$

$$l_{x_M} \approx a \quad [\text{m}] \tag{52}$$

$$l_{y_M} \approx l_p\phi \quad [\text{m}] \tag{53}$$

$$r_{x_M} \approx l_p \quad [\text{m}] \tag{54}$$

$$r_{y_M} \approx l_p\theta \quad [\text{m}] \tag{55}$$

as well as for the components of the matrix M:

$$\boldsymbol{M} = \begin{bmatrix} m_v & m_v b & m_s l_p \\ m_v b & I_v + I_s + m_v b^2 & -I_\theta \\ m_s l_p & -I_\theta & I_\phi \end{bmatrix} \tag{56}$$

and the moments due to the gravity:

$$I_\theta = I_s + m_s l_p a \quad [\text{kg m}^2] \tag{57}$$

$$I_\phi = I_s + m_s l_p^2 \quad [\text{kg m}^2] \tag{58}$$

$$T_{v\theta} \approx 0 \quad [\text{Nm}] \tag{59}$$

$$T_{g\theta} \approx m_s g l_p \phi \quad [\text{Nm}] \tag{60}$$

$$T_{g\phi} \approx m_s g l_p \theta \quad [\text{Nm}] \tag{61}$$

3.2. Proposed form for the power take off moment and feedback law

In view of the non-linear equation of motion (38), the mechanism is inherent to an unstable behaviour. For this reason, a feedback law is incorporated in the power take off moment to ensure static and dynamic stability, being of the following form:

$$T_p = -K_p\phi - R_p\dot{\phi} + T_N \quad [\text{Nm}] \tag{62}$$

where K_p and R_p are constant linear feedback gains to be properly selected and T_N denotes an appropriate compensator for the non-linearity of the system in the form:

$$T_N = \frac{d}{dt}(P_\phi - m_s l_p \dot{u} + I_\theta\dot{\theta} - I_\phi\dot{\phi}) + (T_{g\phi} - m_s g l_p \theta) \quad [\text{Nm}] \tag{63}$$

which results to the following equation for motion of the internal body:

$$I_\phi\ddot{\phi} + R_p\dot{\phi} + K_p\phi = -m_s l_p\ddot{u} + I_\theta\ddot{\theta} - m_s g l_p\theta + T_N \quad [\text{Nm}] \tag{64}$$

Obviously T_N is equal to zero for a linearised system.

3.3. Analysis of the expected dynamic behaviour

Eq. (64) implies that the motion of the internal body is fully equivalent dynamically to that of a damped physical pendulum, with a mass m_s and inertia I_s about its CM, which is suspended at a distance l_p from its centre of mass. However, it should be stretched, that in view of Eq. (47), the equivalent length l_p of this pendulum can be many orders of magnitude higher than that expected by any other vertical pendulum, realised in the traditional natural technological way, as for e.g. in the form of SEAREV. This pendulum can simultaneously convert three different forms of wave energy:

- The kinetic energy resulting from the surge motion.
- The kinetic energy resulting from the pitching motion.
- The potential energy resulting from the pitching motion.

In view of Eq. (62), the selection of the feedback gains can be performed in a way to ensure stability of the system, optimal tuning of the natural periods of the system to the periods of the external source, as well as maximum power conversion capability.

3.4. Calculation of maximum power conversion capacity

The analysis of the power conversion capability can be performed independently for the surge and pitch motion of the converter. However, the design of the external vessel and the coupled form of equations [14] imply that a dependence exists in fact between them. Detailed analysis of such a dependence is performed in [14]. Following the outline of such an analysis, the vessel will be assumed to be subjected to a pitching motion of amplitude Θ_C and frequency ω.

$$\theta(t) = \Theta_C\cos(\omega t) \quad [\text{rad}] \tag{65}$$

while the surge motion will depend on the pitch motion as follows:

$$u(t) = -b\theta(t) = -b\Theta_C\cos(\omega t) \quad [\text{m}] \tag{66}$$

As a result, the equation of motion (64) now becomes:

$$I_\phi\ddot{\phi} + R_p\dot{\phi} + K_p\phi = -M_e\Theta_C\cos(\omega t) \tag{67}$$

where

$$T_p = -K_p\phi - R_p\dot{\phi} \quad [\text{Nm}] \tag{68}$$

$$M_e = \omega^2 I_P + m_s g l_p \quad \left[\text{kg}\left(\frac{\text{m}}{\text{s}}\right)^2\right] \tag{69}$$

$$I_P = I_S + m_s l_p(a+b) \quad [\text{kg m}^2] \tag{70}$$

The steady state response of the system is a harmonic function with a frequency equal to ω and with a phase difference of $\pi/2$ with the excitation force, in order to maximise power capture from the excitation force:

$$\phi(t) = -\Phi_S \sin(\omega t) \quad [\text{rad}] \tag{71}$$

The minus sign is used to denote that for the positive θ angle, a negative ϕ angle should result, in order to ensure the stability of the vessel, meaning that the internal configuration oscillates with a $\pi/2$ phase difference with the external vessel, thus, avoiding collision or overturning. Substitution of Eqs. (58) and (69) into Eq. (67) leads to the following results:

$$R_p = \frac{M_e \Theta_c}{\omega \Phi_s} \quad \left[\text{kg}\frac{\text{m}^2}{\text{s}}\right] \tag{72}$$

$$K_p = \omega^2 I_\phi \quad \left[\text{kg}\left(\frac{\text{m}}{\text{s}}\right)^2\right] \tag{73}$$

The mean power absorbed by the PTO is defined as follows:

$$P_{out} = \frac{1}{T_w}\int_0^{T_w} T_p\dot{\phi}dt \quad [\text{W}] \tag{74}$$

where the wave period is

$$T_w = \frac{2\pi}{\omega} \quad [\text{s}] \tag{75}$$

Substitution of Eqs. (68), (75) into (74) leads to the following expression

$$P_{out} = -\frac{1}{2}\omega M_e \Theta_c \Phi_s = -P_{in} \quad [\text{W}] \tag{76}$$

or alternatively to:

$$P_{out} = -\frac{1}{2}\omega \Theta_c m_s X_M \alpha_e \quad [\text{W}] \tag{77}$$

where:

$$X_M = l_p \Phi_s \quad [\text{m}] \tag{78}$$

$$\alpha_e = g + \omega^2(a+b+l_I) \quad \left[\frac{\text{m}}{\text{s}^2}\right] \tag{79}$$

$$l_I = \frac{I_S}{m_s l_p} \quad [\text{m}] \tag{80}$$

and

- X_M: amplitude of the linear motion of the centre of mass of the oscillating body,
- Φ_s: maximum inclination of the mechanism,
- I_S: inertia of the oscillating body about its *CM*,
- T_w: sea waves period.

In summary, the inclusion of the PTO mechanism with the incorporated feedback law, allows the designer to limit the amplitude of the internal body's angle, by controlling appropriately the damping coefficient of the PTO mechanism. This means that as far as the movement of the internal body is concerned, which is simulated and presented in this paper, the selection of a comparably big excitation pitch amplitude Θ_C, does not violate the assumption of small perturbations used in the linearisation of the equation nor it inserts any significant error between the linearised and the non-linear model.

4. A standalone 750 kW rated power configuration

The wave energy level is expressed as power per unit length along the wave crest or along the shoreline direction. Typical values for "good" offshore locations range between 20 and 70 [kW/m] as annual average and occur mostly in moderate to high latitudes, as for e.g. in the North Sea. A design approach for a peak energy level of 30 [kW/m] (also considering good locations in the Mediterranean Sea) can be reasonably used as a target value to be reached by the subsequent configurations to be designed.

The actual power that can be absorbed by a pitching and surging WEC is expressed by the value of the Capture Width, which is around $L = \lambda/\pi$ [m], for pitching and surging WECs [7]. Assuming a typical value for the wavelength of $\lambda \approx 50:100$ [m], L is calculated. Multiplication of this value with the wave power per unit length, results to a total value of power around $0.5:1$ MW [14], which can be absorbed by a unique WEC. Moreover, assuming the buoy to be of a hemispherical shape, estimates for the optimum radius of the buoy $D_v/2 = R = 0.262T_w^2$ [m] can be derived [7], although this value has been proved for heaving motion only. Taking into account wave periods of 6: 10 s, this leads to buoy with a radius of at least $10:14$ [m], able to capture the amount of power calculated previously. The above estimates are in line with the results found in corresponding sources [23].

Therefore, an indicative mechanism for a standalone 750 [kW] rated configuration is presented. A body consisting of two unequal spheres and a beam that links them together will be used as an inertial mass. This body is suspended with three links inside a sealed vessel. All the other additional components such as the hydraulic system and the rams are also enclosed in the vessel. This basic configuration has the form presented in Figs. 2 and 3. It should be noted, that hydraulic power take of systems can offer a reliable and efficient approach for wave energy conversion [24]. As Figs. 2 and 3 indicate, the vessel is a fully sealed hull with a plate at the bottom for maximiing reaction, increasing the added mass and lowering the cente of mass of the external vessel. The hydraulic system power pack can be placed at the bottom, while the rams operate in the same plane with the cente of mass of the oscillating body capable to absorb motion in any direction without interfering with the suspended body. The final form of the PTO mechanism has to be designed according to the final dimensions and constraints of the device.

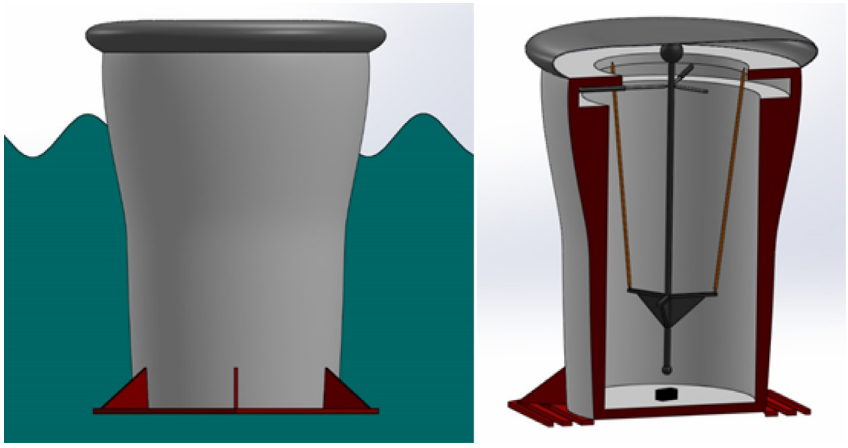

Fig. 2. A fully enclosed multi-axis combined surge and pitch configuration, for wave energy conversion.

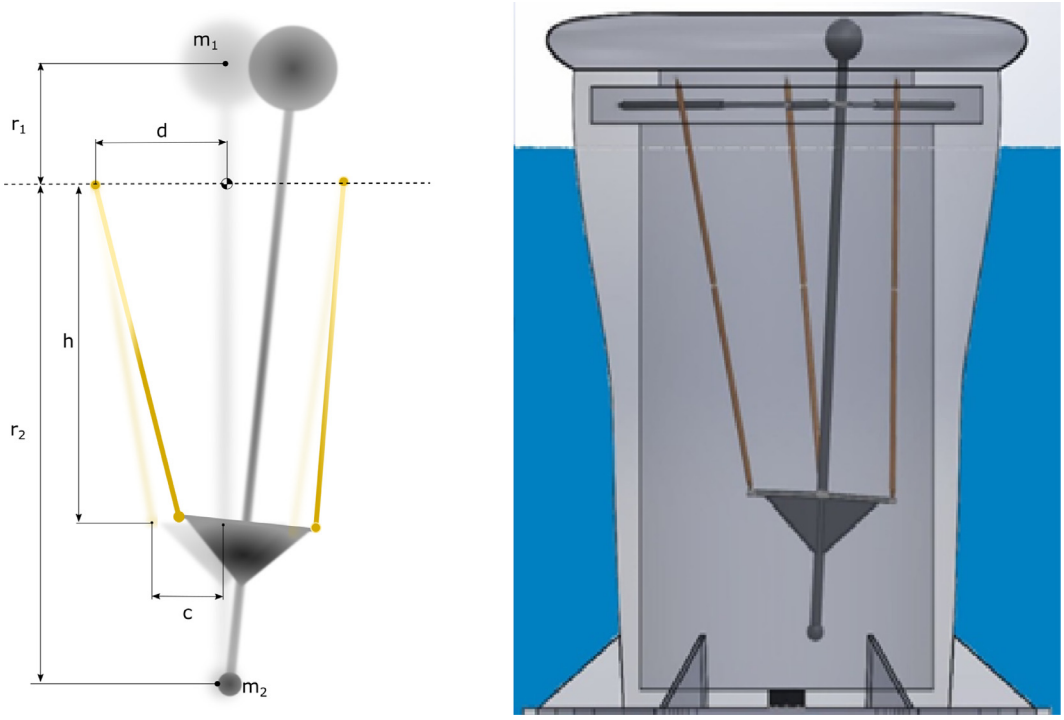

Fig. 3. Rest position and limit position of the inertial mass.

The detailed design of the hull is beyond the scope of this paper, since emphasis is placed on the design of the mechanism itself. However, efficient procedures for its optimal design can be applied [25,26]. The geometry of the final form of the suspended body, is presented in Fig. 3. The first sphere, made of iron, has a radius of $R_1 = 1.13$ [m], while the second $R_2 = 0.62$ [m]. The centres of those two components have a distance of 35 [m]. Assuming that the weight of the beam and the supporting brackets are evenly distributed along the total length, the values of $m_1 = 48$ [tn], $r_1 = 5$ [m] and $m_2 = 8$ [tn] and $r_2 = 30$ [m] are reached, where m_1 and m_2 indicate the masses of the two spheres and r_1, r_2 their distance measured from the cente of mass of the body (pendulum) . Considering that $m_s = m_1 + m_2$ and $m_1/m_2 = r_2/r_1$, the moment of inertia of the body S

$$I_{S_C} = m_s r_1 r_2 \quad [\mathrm{kg\,m^2}] \tag{81}$$

and

$$I_S \equiv I_{S_O} = m_s\left(r_1 r_2 + a^2\right) \quad [\mathrm{kg\,m^2}] \tag{82}$$

The main objective of the paper is to provide a parametric design of the internal oscillating mechanism, in order that this mechanism is able to capture a specific peak (maximum) power. This estimate involves also parameters of the external vessel, such as the dimension D_V, related to the diameter of the vessel, as well as length a, related to the cente of mass of the external vessel, both depending its hydrodynamic characteristics. However, the emphasis of the paper is to evaluate

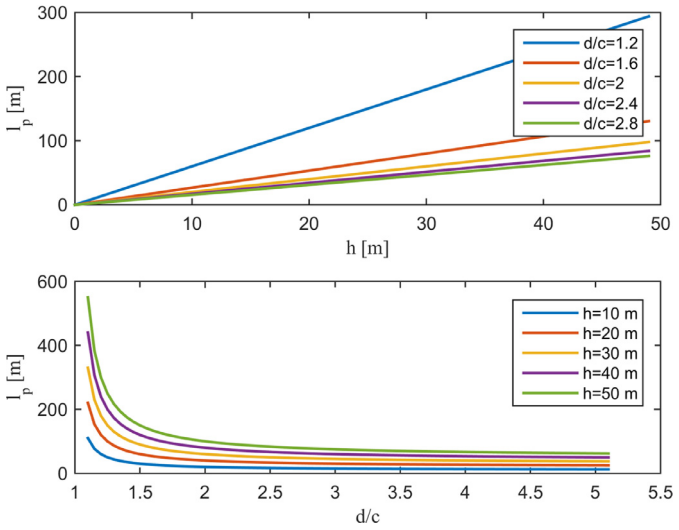

Fig. 4. (a) Equivalent pendulum length l_p for varying values of the ratio d/c. (b) Equivalent pendulum length l_p for varying values of h.

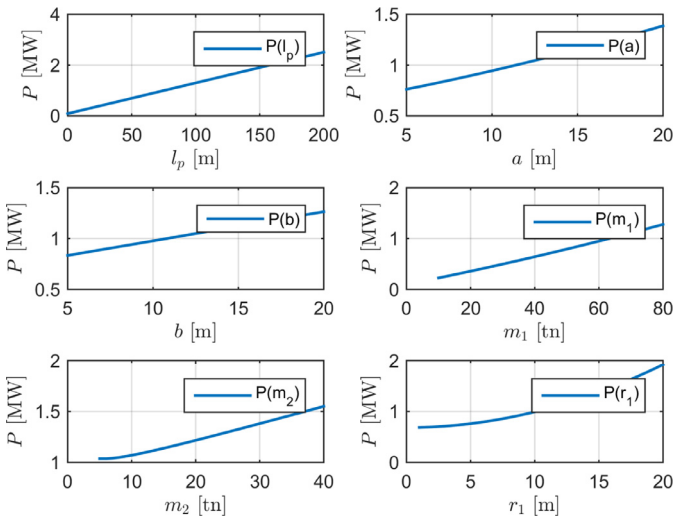

Fig. 5. Contribution of the main parameters of the design and suspended body to the output power.

the effect of the parameters of the internal mechanism on the captured power.

Examination of Eq. (76) of the output power, for different values of the four-bar mechanism's lengths h, d, c, as noted on Fig. 10 and also the masses and distances between the two spheres of the pendulum, has led to the following graphs shown on Figs. 4 and 5. For this task, a preliminary set of geometrical restrictions has been set, by examining the configuration of the system:

- $h > d, c$,
- $h < r_2$, since the CM of the bottom sphere is below the link DE.

Fig. 4 shows how the equivalent pendulum length l_p depends solely on geometrical parameters of the four-bar mechanism, which are the ratio of the lengths d and c and length h. These graphs exemplify the contribution of the suspension geometry and set the layout of dimensioning of the full design. They also lead to the conclusion that for ratios $d/c > 2$ approximately, increase of length h has significantly reduced contribution to the equivalent pendulum length, which allows the choice of a reasonable and practical value for said length. Another observation is that, as the ratio d/c approaches unity $(d = c)$, output power is ascending and that is because tan $\gamma_0 \to \infty$. Of course, this ratio is restricted by the basic geometry of the mechanism and the vessel as a system meaning the calculated diameter of the vessel for the desired power absorption from the waves and a typical average water depth at which the whole configuration is expected to be moored, from which in turn the height of the external vessel (and consequently the height of the suspended body and the suspension geometry) is restricted.

Table 1
Main design parameters of the standalone 750 kW power rated configuration, for both pitch and surge excitation.

Four-bar mechanism

h [m]	d [m]	c [m]	γ_0 [°]	l [m]	μ	l_p [m]
20.00	6.25	4.00	83.58	20.13	1.78	55.56

Body and Vessel

m_1 [tn]	m_2 [tn]	r_1 [m]	r_2 [m]	a [m]	b [m]
48.00	8.00	5.00	30,00	5,00	2,50
m_s [kg]	I_s [kgm^2]	I_p [kgm^2]	I_ϕ [kgm^2]	D_V [m]	–
5.60×10^4	9.80×10^7	3.31×10^7	1.83×10^8	33.54	–

Response parameters

Θ_c [°]	Φ_s [°]	T_w [s]	ω [rad/s]	M_e [kgm^2/s^2]	X_M [m]
25.00	5.00	8.00	0.79	5.10×10^7	4.85

PTO

R_p	K_p	P_{out} [kW]
3.24×10^8	1.13×10^8	760

The linear correlation between the output power and the equivalent pendulum length l_p, is obvious in Eq. (76) which is also shown in Fig. 5. The same stands for the total mass m_s. Definitely, l_p is the most notable contributor in the total power conversion capability of the system, especially taking into consideration the practical aspects in implementing the corresponding magnitudes of each variable.

In Table 1, an indicative set of dimensions of the suspension geometry and parameters of the suspended body are presented, under the previously assumed surging and pitching excitation, which result to an approximate 750 [kW] rating of power capability for this concept. As far as hydrodynamic parameters are concerned, all the assumed values are in accordance to the sources [10,14], taking into consideration similar implementations and environmental scenarios.

It should be clarified, that the above values refer just to an indicative implementation of a mechanism for wave energy conversion and they are by no means optimied. Such

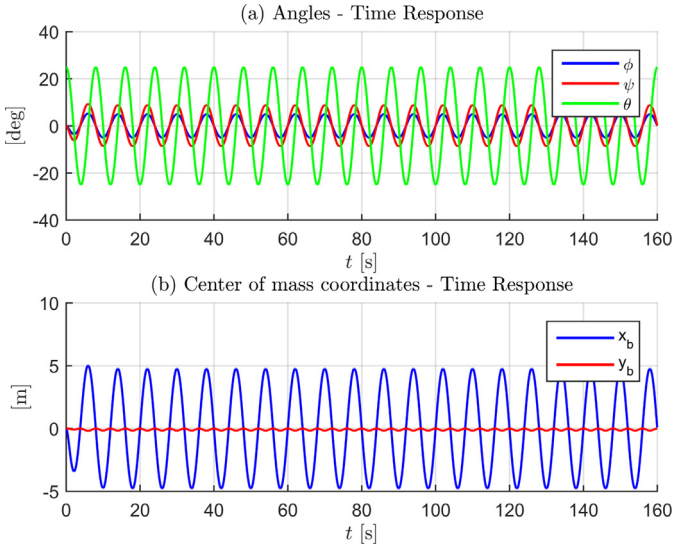

Fig. 6. (a) Response of the angles ϕ, θ, ψ for harmonic excitation of the system (b) Movement of the body's centre of mass C, according to the RX_bY_b coordinate system during the excitation.

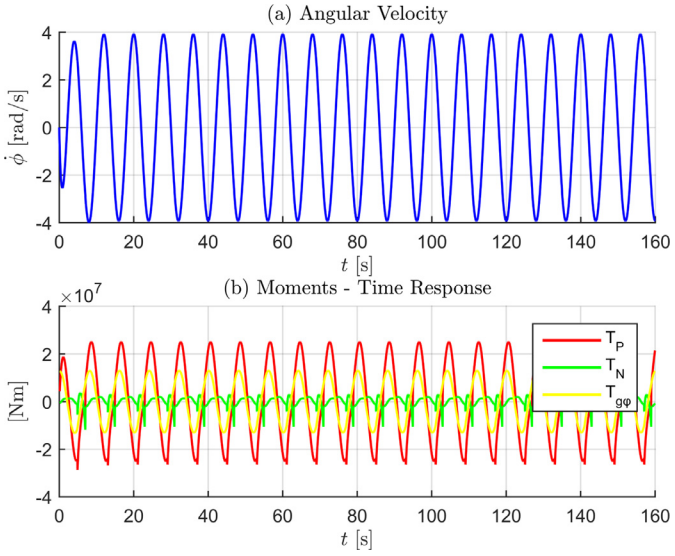

Fig. 7. (a) Response of the angular velocity $\dot{\phi}$ (b) Response of the output moments of the system.

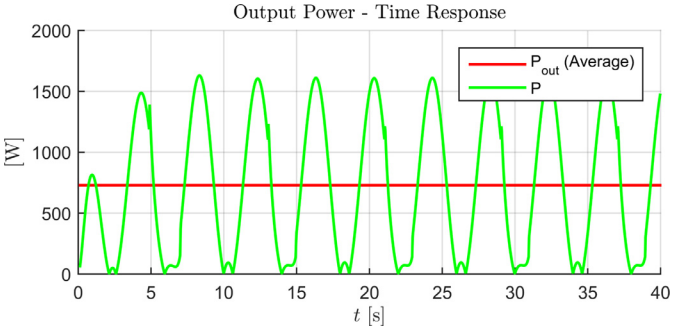

Fig. 8. Response of the output power and the time average output power.

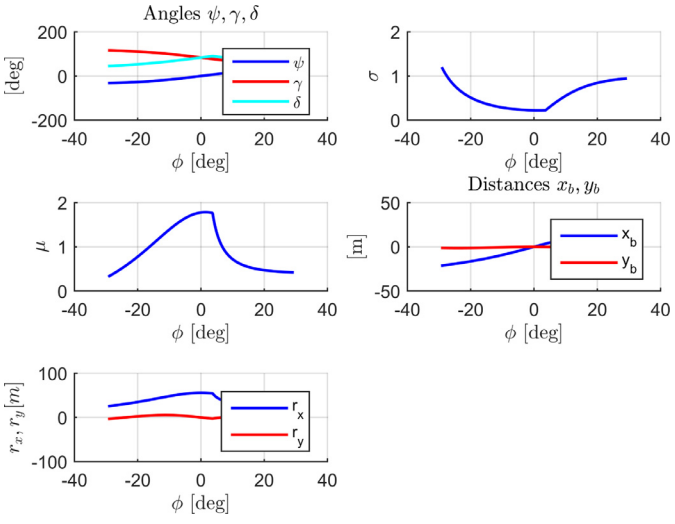

Fig. 9. (a) Angles ψ, γ and δ as a function of angle ϕ. (b) Dimensionless parameter σ as a function of angle ϕ. (c) Dimensionless parameter μ as a function of angle ϕ. (d) Coordinates of the body's S centre of mass C, as a function of angle ϕ. (e) Parameters r_x and r_y, which express the relation between the velocities of point C and angular velocity $\dot{\phi}$, as a function of angle ϕ.

an approach is obviously necessary in full association to the design of an optimied external vessel. The combined values of power and suspended mass in Table 1 compare more than favourably to those necessary for other types of internally reacting WECs, such as PSFrog [14] SEAREV [13,26] or other technologies [27]. Far more important, the suspension geometry and the simplicity of the PTO mechanism, render this design far more reliable and easily implementable than all other known types of internally reacting masses.

Next, using the non-linear form of the system of equations for the internal body, are presented the diagrams showing the response of angles ϕ, θ, ψ, the movement of point C, the angular velocity $\dot{\phi}$, and the output moments.

In Fig. 6(a), the responses of the angle ψ is presented along with the external vessel's pitch angle θ and the suspended body's angle ϕ. Of course, the amplitudes of θ and ϕ are set according to Section 3.4. The response of of the angle ψ, essentially reveals the divergence of the link AD from its rest position and how the possibility of collision or overturn of the external vessel is avoided due to the phase difference with the excitation. Fig. 6(b), demonstrates the almost completely linear motion of the cente of mass of the suspended body since the amplitude of the response of y_b is relatively extremely small, even when simulating the non-linear form of the equation of the internal body. Fig. 7 shows the response of the angular velocity of the suspended body and below the developing output moments of the PTO mechanism, the compensator in the non-linear case and the gravity component respectively. Fig. 8 shows the time response of the output power converted by the internal configuration along with the time average output power which is the corresponding nominal rating of the design.

Fig. 9 shows how various geometric parameters of the system, respond as functions of angle ϕ. It is worth noting that for small perturbations of the angle ϕ, parameters like μ, σ,

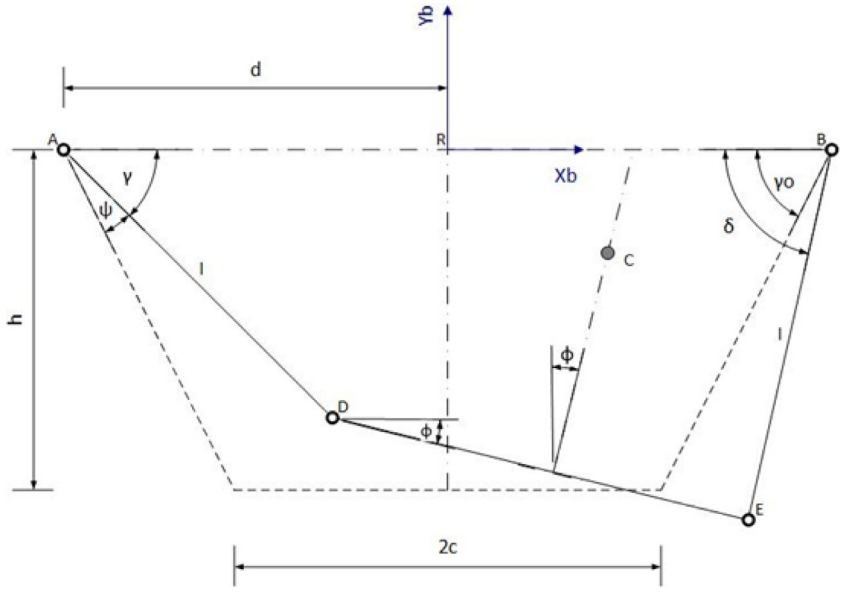

Fig. 10. Geometric parameters and kinematic variables of the four-bar mechanism.

r_x, r_y and the angles ψ, γ, δ remain approximately constant, which showcases the validity of the assumption of small perturbations during the linearisation of the model.

5. Conclusion

This concept of wave energy conversion, using fully enclosed inertially reacting bodies under appropriate suspension geometry from an external floating vessel, can provide a reliable and simple design, able to meet the severe conditions for survivability under extreme weather conditions. As it results, the linear motion of the cente of mass of the suspended body enables the introduction of a quite simple form of a PTO design. Moreover, the simplicity and the symmetry of the suspension geometry and of the PTO mechanism, ensure a quite simple and robust technological implementation. Moreover, the optimal dynamic design of the geometry and the mass and the inertia distribution of the internal body ensure the maximal conversion and storage of the wave energy. This results to a significant reduction of the suspended mass, compared to other internal reacting designs. Also, the mass and the inertia distribution of the internal body is optimied, ensuring the maximal conversion and storage of the wave energy in the form of kinetic and potential energy. As a result, the dynamic behaviour of the internal body assembly is essentially that of an equivalent vertical physical pendulum. However, the resulting equivalent pendulum length and inertia can far exceed those that can be achieved by an actual technical implementation either of a simple horizontal or of a vertical pendulum (suspended, or inverted), with a direct consequence to a significant reduction of the suspended mass. The concept is flexible and parametrically designed, enabling its implementation in any form of floating vessels. A first option is as standalone WECs, fully enclosed in appropriately designed hulls. Moreover, an alternative direction for their implementation consists in properly embedding them in floating offshore platforms, supporting wind turbines. Such a design can drastically enhance the performance, the efficiency and the potential of floating offshore energy applications.

Appendix A

A1. Kinematic analysis of the four-bar mechanism

Geometric parameters

The basic geometrical configuration of the mechanism is defined by the selection of the three independent lengths , , . The rest of the geometric parameters can be retrieved as follows:

$$l = \sqrt{(d-c)^2 + h^2} \quad [\mathrm{m}] \tag{A.1}$$

$$\tan\gamma_0 = \frac{h}{d-c} \tag{A.2}$$

Reference position of the mechanism

The reference (rest) position of the mechanism, indicated by dashed lines, is defined by the following relations:

$$\phi = \psi = 0 \quad [rad], \quad \gamma = \delta = \gamma_0 \quad [\mathrm{rad}] \tag{A.3}$$

The origin of the coordinate system RX_bY_b is selected in the middle of the stationary link (ground) of the mechanism, with the position of the axes indicated as in the figure. Relations between the angles of the mechanism. The kinematics of the mechanism can be fully retrieved as a function of a single degree of freedom: the angle ϕ. he rest of the angles can be retrieved by the following compatibility relations of the closed kinematic chain:

$$l\cos\gamma + 2c\cos\phi + l\cos\delta = 2d \quad [\mathrm{m}] \tag{A.4}$$

$$l\sin\gamma + 2c\sin\phi - l\sin\delta = 0 \quad [\mathrm{m}] \tag{A.5}$$

Reforming the above equations, the following system is obtained:

$$l\cos\delta = 2d - l\cos\gamma - 2c\cos\phi \quad [\mathrm{m}] \tag{A.6}$$

$$l\sin\delta = l\sin\gamma + 2c\sin\phi \quad [\mathrm{m}] \tag{A.7}$$

Using the following abbreviations,

$$x_\phi = d - c\cos\phi \quad [\mathrm{m}] \tag{A.8}$$

$$y_\phi = c\sin\phi \quad [\mathrm{m}] \tag{A.9}$$

$$r_\phi = x_\phi^2 + y_\phi^2 \quad [\mathrm{m}^2] \tag{A.10}$$

After squaring each of the above equations and adding them:

$$l^2 = (2x_\phi - l\cos\gamma)^2 + (2y_\phi + l\sin\gamma)^2 \tag{A.11}$$

which results to:

$$-x_\phi l\cos\gamma + y_\phi l\sin\gamma + r_\phi = 0 \tag{A.12}$$

This equation can be further recast to second order polynomial equation

$$\alpha_{2\phi} z_\gamma^2 + 2\alpha_{1\phi} z_\gamma + \alpha_{0\phi} = 0 \tag{A.13}$$

where

$$z_\gamma = tan(\gamma/2) \tag{A.14}$$

$$a_{2\phi} = r_\phi + x_\phi l \quad [\mathrm{m}^2] \tag{A.15}$$

$$a_{1\phi} = y_\phi l \quad [\mathrm{m}^2] \tag{A.16}$$

$$a_{0\phi} = r_\phi - x_\phi l \quad [\mathrm{m}^2] \tag{A.17}$$

which can lead to the definition of the angle γ as a function of the angle ϕ.

$$\gamma = 2\tan\left(\frac{-a_1\phi + \Delta}{a_2\phi}\right)^{-1} \quad [\mathrm{rad}] \tag{A.18}$$

$$\Delta = \sqrt{a_{1\phi}^2 - a_{2\phi}a_{0\phi}} \quad [\mathrm{m}^2] \tag{A.19}$$

The rest of the angles can be then obtained as follows:

$$\psi = \gamma_0 - \gamma \quad [\mathrm{rad}] \tag{A.20}$$

$$\delta = \sin\left(\sin\gamma + \frac{2c}{l}\sin\phi\right)^{-1} \quad [\mathrm{rad}] \tag{A.21}$$

Angular velocities

The time derivatives of the compatibility relations of the closed kinematic chain (A.4) and (A.5), lead to the following equations:

$$-l\dot{\gamma}\sin\gamma - 2c\dot{\phi}\sin\phi - l\dot{\delta}\sin\delta = 0 \tag{A.22}$$

$$l\dot{\gamma}\cos\gamma + 2c\dot{\phi}\cos\phi + l\dot{\delta}\cos\delta = 0 \tag{A.23}$$

These can be further processed as following:

$$l\dot{\delta}\sin\delta = -l\dot{\gamma}\sin\gamma - 2c\dot{\phi}\sin\phi \tag{A.24}$$

$$l\dot{\delta}\cos\delta = l\dot{\gamma}\cos\gamma + 2c\dot{\phi}\cos\phi \tag{A.25}$$

or

$$l\dot{\delta}\cos\delta\tan\delta = -l\dot{\gamma}\sin\gamma - 2c\dot{\phi}\sin\phi \tag{A.26}$$

$$l\dot{\delta}\cos\delta\tan\delta = (l\dot{\gamma}\cos\gamma + 2c\dot{\phi}\cos\phi)\tan\delta \tag{A.27}$$

Combining Eqs. (A.26) and (A.27) together the following relations are obtained:

$$(l\dot{\gamma}\cos\gamma + 2c\dot{\phi}\cos\phi)\tan\delta = -l\dot{\gamma}\sin\gamma - 2c\dot{\phi}\sin\phi \Leftrightarrow \tag{A.28}$$

$$\sin\delta(l\dot{\gamma}\cos\gamma + 2c\dot{\phi}\cos\phi) = \cos\delta(-l\dot{\gamma}\sin\gamma - 2c\dot{\phi}\sin\phi) \Leftrightarrow \tag{A.29}$$

$$\dot{\gamma} l sin(\gamma + \delta) = -\dot{\phi} 2c\sin(\phi + \delta) \tag{A.30}$$

Which can be finally expressed in the following compact form:

$$\dot{\gamma} = -\frac{2c}{l\sigma}\dot{\phi} = -\mu\dot{\phi} \quad [\mathrm{rad/s}] \tag{A.31}$$

$$\dot{\psi} = -\dot{\gamma} = \mu\dot{\phi} \quad [\mathrm{rad/s}] \tag{A.32}$$

$$\mu = \frac{2c}{l\sigma} \tag{A.33}$$

$$\sigma = \frac{\sin(\gamma + \delta)}{\sin(\phi + \delta)} \tag{A.34}$$

Motion of the cente of mass

The original position of the cente of mass C of a body attached to the mechanism is assumed to coincide with the origin R of the coordinate system RX_bY_b at the rest position of the mechanism. Therefore, its coordinates x_B, y_B with respect to this system at an arbitrary position of the mechanism can be derived as follows:

$$x_B = -d + l\cos\gamma + c\cos\phi + h\sin\phi \quad [\mathrm{m}] \tag{A.35}$$

$$y_B = l\sin\gamma + c\sin\phi - h\cos\phi \quad [\mathrm{m}] \tag{A.36}$$

$$h = l\sin\gamma_0 \quad [\mathrm{m}] \tag{A.37}$$

It is easy to derive that y_B is equal to zero when $l = 2d = 4c$, as it is the special case of the Roberts linkage. Therefore, the point moves in a straight line over the segment AB. The velocities of C can be derived as follows:

$$\dot{x}_B = -l\dot{\gamma}\sin\gamma - c\dot{\phi}\sin\phi + h\dot{\phi}\cos\phi \quad [\mathrm{m/s}] \tag{A.38}$$

$$\dot{y}_B = l\dot{\gamma}\cos\gamma + c\dot{\phi}\cos\phi + h\dot{\phi}\sin\phi \quad [\mathrm{m/s}] \tag{A.39}$$

or, in view of Eq. (A.31)

$$\dot{x}_B = (l\mu\sin\gamma - c\sin\phi + h\cos\phi)\dot{\phi} \quad [\mathrm{m/s}] \tag{A.40}$$

$$\dot{y}_B = (-l\mu\cos\gamma + c\cos\phi + h\sin\phi)\dot{\phi} \quad [\mathrm{m/s}] \tag{A.41}$$

and finally in the following compact form:

$$\dot{x}_B = r_x\dot{\phi} \quad [\mathrm{m/s}] \tag{A.42}$$

$$\dot{y}_B = r_y\dot{\phi} \quad [\mathrm{m/s}] \tag{A.43}$$

where:

$$r_x = l\mu\sin\gamma - c\sin\phi + h\cos\phi \quad [\mathrm{m}] \tag{A.44}$$

$$r_y = -l\mu\cos\gamma + c\cos\phi + h\sin\phi \quad [\mathrm{m}] \tag{A.45}$$

A2. Derivatives of the Lagrangian function

The Lagrangian of the system is defined as follows:

$$L = T - U \tag{A.46}$$

where the expressions for the kinetic energy and of the potential energy are defined in Eqs. (15) and (16). The system has three degrees of freedom:

$$\mathbf{r} = \begin{Bmatrix} u & \theta & \phi \end{Bmatrix}^T \tag{A.47}$$

$$\dot{\mathbf{r}} = \begin{Bmatrix} \dot{u} & \dot{\theta} & \dot{\phi} \end{Bmatrix}^T \tag{A.48}$$

The derivatives of the Lagrangian function for the kinetic energy part are:

$$\begin{aligned} \frac{\partial L}{\partial \dot{u}} &= \frac{\partial T}{\partial \dot{u}} \\ &= m_v \dot{x}_G \frac{\partial \dot{x}_G}{\partial \dot{u}} + m_v \dot{x}_M \frac{\partial \dot{x}_M}{\partial \dot{u}} \\ &= m_v \dot{x}_G + m_s \dot{x}_M \\ &= (m_v + m_s)\dot{u} + (m_v b \cos\theta - m_s l_{x_M})\dot{\theta} + m_s r_{x_M}\dot{\phi} \end{aligned} \tag{A.49}$$

$$\begin{aligned} \frac{\partial L}{\partial \dot{\theta}} &= \frac{\partial T}{\partial \dot{\theta}} \\ &= I_v\dot{\theta} + I_s(\dot{\theta} - \dot{\phi}) + m_v \dot{x}_G + m_v \dot{y}_G \frac{\partial \dot{y}_G}{\partial \dot{\theta}} + m_s \dot{x}_M \frac{\partial \dot{x}_M}{\partial \dot{\theta}} \\ &\quad + m_s \dot{y}_M \frac{\partial \dot{y}_M}{\partial \dot{\theta}} \\ &= I_v\dot{\theta} + I_s(\dot{\theta} - \dot{\phi}) + m_v(\dot{u} + b\dot{\theta}\cos\theta)b\cos\theta \\ &\quad + m_v b\dot{\theta}\sin\theta b\sin\theta \\ &\quad + m_s(\dot{u} - l_{x_M}\dot{\theta} + r_{x_M}\dot{\phi})(-l_{x_M}) + m_s(l_{y_M}\dot{\theta} + r_{y_M}\dot{\phi})l_{y_M} \\ &= (m_v b\cos\theta - m_s l_{x_M})\dot{u} + [I_v + I_s + m_v b^2 \\ &\quad + m_s(l_{x_M}^2 + l_{y_M}^2)]\dot{\theta} - [I_s + m_s(r_{x_M} l_{x_M}) - r_{y_M} l_{y_M}]\dot{\phi} \end{aligned} \tag{A.50}$$

$$\begin{aligned} \frac{\partial L}{\partial \dot{\phi}} &= \frac{\partial T}{\partial \dot{\phi}} = I_s(\dot{\theta} - \dot{\phi}) + m_s \dot{x}_M \frac{\partial \dot{x}_M}{\partial \dot{\phi}} + m_s \dot{y}_M \frac{\partial \dot{y}_M}{\partial \dot{\phi}} \\ &= m_s(\dot{u} - l_{x_M}\dot{\theta} + r_{x_M}\dot{\phi})r_{x_M} + m_s(l_{y_M}\dot{\theta} + r_{y_M}\dot{\phi})r_{y_M} \\ &\quad + I_s(\dot{\theta} - \dot{\phi}) \\ &= m_s r_{x_M}\dot{u} - [I_s + m_s(r_{x_M} l_{x_M} - r_{y_M} l_{y_M})]\dot{\theta} \\ &\quad + [I_s + m_s(r_{x_M}^2 + r_{y_M}^2)]\dot{\phi} \end{aligned} \tag{A.51}$$

The derivatives of the Lagrangian function for the potential energy part are:

$$\frac{\partial L}{\partial u} = \frac{\partial T}{\partial u} = 0 \quad [\mathrm{N}] \tag{A.52}$$

$$\frac{\partial L}{\partial \theta} = \frac{\partial T}{\partial \theta} = K_v\theta + m_v g b \sin\theta + m_s g l_{y_M} \quad [\mathrm{Nm}] \tag{A.53}$$

$$\frac{\partial L}{\partial \phi} = \frac{\partial T}{\partial \phi} = m_s g r_{y_M} \quad [\mathrm{Nm}] \tag{A.54}$$

The expressions for l_{x_M}, l_{y_M}, r_{x_M}, r_{y_M} are defined in equations Eqs. (11)–(14).

References

[1] K. Gunn, C. Stock-Williams, Renew. Energy 44 (2012) 296–304.
[2] D.S. Richardson, G.A. Aggidis, Ocean Renew. Energy 8 (2013).
[3] R. Bedard, G. Hagerman, Offshore Wave Power Feasibility Demonstration Project: Project Definition Study, Final Summary Report, EPRI, 2005.
[4] A. Athanasia, A.-B. Genachte, Deep Water: The Next Step for Offshore Wind Energy, 2013 URL http://www.ewea.org/fileadmin/files/library/publications/reports/Deep_Water.pdf.
[5] L. Serri, A. Sempreviva, T.Pontes, J. Murphy, K. Lynch, D. Airoldi, J. Hussey, C. Rudolph, I. Karagali, 2012. Resource Data and GIS Tool: For Offshore Renewable Energy Projects in Europe, URL http://www.orecca.eu/c/document_library/get_file?uuid=757326c6-102f-4dd3-8790-916755694103&groupId=10129.
[6] B. Drew, A. Plummer, M.N. Sahinkaya, Proc. Inst. Mech. Eng. Part A J. Power Energy 223 (8) (2009) 887–902.
[7] A.F. de O. Falcão, Renew. Sustain. Energy Rev. 14 (3) (2010) 899–918.
[8] K. Lynch, J. Murphy, 2012. Deliverable d3.6: Overview of Offshore Wind and Ocean Energy Technologies, URL http://www.marina-platform.info/dissemination.aspx.
[9] R. Bracewell, Frog and PS Frog: A Study of two Reactionless Ocean Wave Energy Converters, Ph.D. thesis, Lancaster University, UK, 1990.
[10] A. McCabe, A. Bradshaw, J. Meadowcroft, G. Aggidis, Renew. Energy 31 (2) (2006) 141–151.
[11] U. Korde, Appl. Ocean Res. 21 (5) (1999) 235–248.
[12] U.A. Korde, Appl. Ocean Res. 23 (5) (2001) 251–262.
[13] A. Babarit, A. Clement, J. Gilloteaux, in: Proceedings of the Twenty-fourth International Conference on Offshore Mechanics and Arctic Engineering, Halkidiki, Greece, vol. 2, 2005, pp. 703–712.
[14] M.B. Widden, M.J. French, G.A. Aggidis, Proc. Inst. Mech. Eng. Part M J. Eng. Marit. Environ. 222 (2008) 153–161.
[15] W. Ltd., The Penguin Wave Energy Converter, 2015.
[16] EERE, Wave energy prize, URL http://waveenergyprize.org/, Online; accessed Oct-2016.
[17] D. Zhang, G. Aggidis, Y. Wang, A. Mccabe, W. Li, Appl. Phys. Lett. 103 (10) (2013).
[18] F. Salcedo, P. Ruiz-Minguela, R. Rodriguez, P. Ricci, M. Santos, in: Proceedings of the Eighth European Wave Tidal Energy Conference, 2009, p. 4605.
[19] T. Perez, M. Santos-Mujica, J.P. Ruiz-Minguela, in: Proceedings of the 2009 European Control Conference (ECC), 2009, pp. 3743–3748.
[20] H. Kanki, S. Arii, T. Furusawa, T. Otoyo, in: Proceedings of the Eighth European Wave and Tidal Energy Conference, 2009.
[21] G. Waizmann, The Wave Gyro, Master thesis, University of Southampton, UK, 2011.
[22] G. Bracco, E. Giorcelli, G. Mattiazzo, Mech. Mach. Theory 46 (10) (2011) 1411–1424.
[23] A. Babarit, Renew. Energy 80 (2015) 610–628.
[24] J.F. Gaspar, M. Calvrio, M. Kamarlouei, C.G. Soares, Renew. Energy 86 (2016) 1232–1246.
[25] A. McCabe, Renew. Energy 51 (2013) 274–284.
[26] J. Cordonnier, F. Gorintin, A.D. Cagny, A. Clment, A. Babarit, Renew. Energy 80 (2015) 40–52.
[27] M. Mekhiche, K.A. Edwards, in: Proceedings of the Second Marine Energy Technology Symposium, Seattle, WA, USA, 2014.